nonhomogeneous sub-domain in the first iteration and afterwards, the iterative procedure is applied in the same way as presented in Ref. 5 for plane wave scattering. It has shown that the main characteristics of the IMR technique are independent of the numerical method used in each sub domain. It shows that when the coupling between the regions increases, not only the number of iterations but also the inaccuracy of the procedure increase. In most cases, to overcome this disadvantage, the reduction of the domain discretization can be enough. Although in this article the iterative method was presented for a problem domain with two regions, its application for multiple domains with multiple sources is straightforward. Also, the error bounds and convergence rate are independent of the number of subdomains.

ACKNOWLEDGMENTS

This work was partially supported by CNPq (Grant 350902/1997–6).

REFERENCES

1. B. Despres, Domain decomposition method and the Helmholtz problem, Proceedings of International Symposium on Mathematics and Numericals, Strasbourg, France, 1992.
2. S. Kurz, J. Fetzer, and G. Lehner, An improved algorithm for the BEM-FEM-coupling method using domain decomposition, IEEE Trans Magn 31 (1995), 1737–1740.
3. A.C. Polycarpou and C.A. Balanis, Finite-element domain decomposition using an iterative approach: Computation of mutual coupling, IEEE Antennas Propag 2 (2000), 1164–1167.
4. R.J. Burkholder and T. Lundin, Forward-backward iterative physical optics algorithm for computing the RCS of open-ended cavities, IEEE Trans Antennas Propag 53 (2005), 793–799.
5. M.H. Al Sharkawy, V. Demir, and A.Z. Elsherbeni, Plane wave scattering from three dimensional multiple objects using the iterative multiregion technique based on the FDFD method, IEEE Trans Antennas Propag 54 (2006), 666–673.
6. R. Adriano, M. Afonso, R. Pires, C. Rego, J.A. Vasconcelos, J.O. Paulino, M. Schroeder, A. Rabello, and T. Oliveira, Iterative method applied to solve electromagnetic susceptibility problems, 12th Biennial IEEE CEFC, 2006, pp. 323–323.
7. M. Carr and J.L. Volakis, A generalized framework for hybrid simulation of multi-component structures using iterative field refinamente, IEEE Trans Antennas Propag 48 (2006), 22–32.
8. J. Jin, The finite element method in electromagnetics, Wiley, New York, 2002.
9. J. Wang, Generalized moment methods in electromagnetics, Wiley, New York, 1938.
10. A. Voors, 4NEC2—-A powerful free NEC antenna analysis package, February 2006, Available at http://home.ict.nl/ arivoors/

© 2007 Wiley Periodicals, Inc.

DESIGN OF WIDEBAND HIGH AND LOW IMPEDANCE METATRANSMISSION LINES

J. Perruisseau-Carrier and A. K. Skrivervik
Laboratory of Electromagnetics and Acoustics (LEMA), Ecole Polytechnique Fédérale de Lausanne (EPFL), Switzerland

Received 27 December 2006

ABSTRACT: *The modeling and design of "metamaterial " composite right/left handed transmission lines (CRLH-TL) is usually based on the assumption that its unit cell is small in terms of the host TL wavelength ($d \ll\ll \lambda_0$). However, it was also shown that this assumption is not required for most CRLH-TL applications and difficult to meet for balanced CRLH-TLs in particular cases. Thus, a more general design strategy, free of this assumption, has been implemented. In this letter, we further develop this second approach to show that it allows designing CRLH-TLs whose impedance is much beyond the range achievable in the case where $d \ll \lambda_0$, for a given technology and fabrication tolerances. The use of the presented concept is illustrated by means of a quartz-integrated CRLH-TL exhibiting a low-impedance (20 Ω). Measured results are in good agreement with the theory and satisfactory performances are observed on a bandwidth covering almost the entire K_u band. Potential applications of the presented results are also discussed in a dedicated section.* © 2007 Wiley Periodicals, Inc.

Microwave Opt Technol Lett 49: 1926–1929, 2007; Published online in Wiley InterScience (www.interscience.wiley.com). DOI 10.1002/mop.22628

Key words: *bloch wave; composite right/left handed transmission line (CRLHTL); metamaterial*

1. INTRODUCTION

Metamaterial TLs with extreme impedance values have recently been studied in [1]. These were implemented using a microstrip line with complementary split-ring resonators (CSRR) etched in the ground plane. The present letter also concerns the design of especially high or low-impedance metamaterial TLs, but in the case of an implementation based on the well-known CRLH-TL structure [2–5]. Although the CSRR approach allows designing TLs with a very wide range of impedance at a given frequency, the impedance obtained is strongly frequency-dependent. This is due to the resonant nature of the CSRR and severely limits the bandwidth (BW). In contrast, the CRLH-TL is a nonresonant structure, and we show here that an appropriate design approach—free from the "homogeneous media " assumption $d \ll \lambda_0$ usually employed for CRLH-TL [2, 3]—allows designing CRLH-TL with an impedance beyond the range achievable using conventional design, and this on a very wide BW. Finally, the CRLH-TL low/high-impedance TLs present the advantage of the particular CRLH-TL dispersion characteristic, which has been extensively employed to implement very interesting microwave CRLH-TL-based devices (e.g [2–4]).

This letter is organized as follows: the first part of Section 2 recalls the final results of developments concerning the Bloch wave-based modeling of CRLH-TL, which were presented in detail by the authors in [5]. Based on these results, we then show theoretically that the Bloch impedance at the frequency of 0° phase shift of a balanced CRLH-TL metamaterial is always higher or lower than the impedance of the host TL of the structure, depending on the choice of the reference planes of the CRLH-TL unit cell. The last part of Section 2 explains how to select the right reference planes and provide analytical formulas to control the Bloch impedance of the structure. It is then shown that the method allows overcoming the limitations in terms of impedance that occur using existing modeling methods based on the $d \ll \lambda_0$ assumption. In Sections 4, we discuss possible applications of the results and provide a concrete design example in Section 5, comparing circuit model, full-wave, and measured results.

2. THEORY

2.1. General Developments

Figure 1 shows two possible symmetrical unit cells that can be periodically cascaded to realize CRLH-TLs. First, let us recall that (1)—usually referred to as the balanced condition—links the parameters of the circuits of Figure 1 so that a continuous phase shift is obtained around a frequency of 0° phase shift [2, 4]. This frequency, denoted here as f_0, corresponds to the transition be-

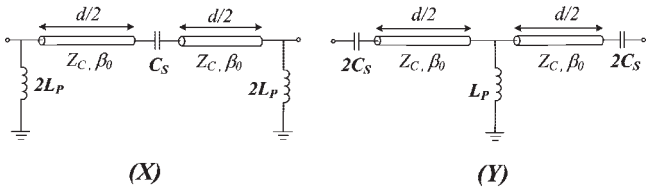

Figure 1 Types X and Y unit cell circuits for 1D CRLH-TLs. Rem: The original drawing file is black on white background. The inversion is due to "manscript central"

tween left and right handed bands of the CRLH-TL. If the balanced condition is met, f_0 is located at the desired frequency by choosing the appropriate host TL length using (2) [4].

$$Z_C = \sqrt{L_P/C_S} \tag{1}$$

$$\beta_0\left(\frac{d}{2}\right) = \frac{1}{2}\arccos\left(\frac{4L_PC_S\omega_0^2 - 1}{4L_PC_S\omega_0^2 + 1}\right) \tag{2}$$

where $\omega_0 = 2\pi f_0$ and β_0 is the propagation constant of the unloaded TL sections at f_0. The Bloch wave impedance of the balanced CRLH-TLs is then calculated using $Z_{equ} = \pm\sqrt{B/C}$, where B and C are elements of the unit cell transmission (ABCD) matrix. Since we want here to match the structure around f_0, we calculate the impedances $Z_{equ,X}$ and $Z_{equ,Y}$ at f_0, which yields:

$$Z_{equ,X}(f_0) = \frac{2L_P\omega_0}{\sqrt{4C_SL_P\omega_0^2 + 1}} \tag{3}$$

$$Z_{equ,Y}(f_0) = \frac{\sqrt{4C_SL_P\omega_0^2 + 1}}{2C_S\omega_0} \tag{4}$$

As demonstarted in [4], a balanced CRLH-TL is only effectively homogenous regarding the modeling of the propagation in the structure—which means that the size of the unit cell d is small in terms of host TL wavelength λ_0 ($d \ll \lambda_0$)—if the following condition on the circuit parameters is met:

$$4L_PC_S\omega_0^2 \gg 1 \tag{5}$$

Here, (1)–(4) are free of any assumption with respect to the circuits of Figure 1 and thus do not rely on the aforementioned assumption. It is nevertheless interesting to note that in the "conventional " case $d \ll \lambda_0$, the Bloch wave impedance at f_0 tends toward the impedance of the unloaded TL. Indeed, making use of (4a) and the balanced condition (1) in (3) and (4) yields

$$Z_{equ,X/Y}(f_0) = Z_C \tag{6}$$

2.2. Particular Properties of the CRLH-TL Bloch Impedance

Considering now again the general case of concern here and multiplying (3) by (4) while making use of (1), we obtain

$$Z_{equ,X}(f_0) \cdot Z_{equ,Y}(f_0) = Z_C^2 \tag{7}$$

Dividing now (3) by (4) and considering that lumped elements values and frequency are always positive, we get:

$$\frac{Z_{equ,X}(f_0)}{Z_{equ,Y}(f_0)} = \frac{4C_SL_P\omega_0^2}{4C_SL_P\omega_0^2 + 1} < 1 \tag{8}$$

Finally, combining (7) and (8), we deduce:

$$Z_{equ,Y}(f_0) > Z_C > Z_{equ,X}(f_0) \tag{9}$$

3. DESIGN OF HIGH/LOW IMPEDANCE CRLH-TLs

A CRLH-TL with a given impedance Z_G at f_0 —determined by the application (see Section 4)—is obtained by enforcing $Z_{equ,X}(f_0) = Z_G$ or $Z_{equ,Y}(f_0) = Z_G$ for circuits X or Y, respectively. A linear design procedure using closed form expressions was presented in [5]. This method can be applied to design the CRLH-TLs with high and low-impedance Z_G concerned here, provided that the following points, resulting from the above developments, are observed:

i. Result (9) means that a CRLH-TL of type X (resp. Y) will always exhibit a lower (resp. higher) impedance Z_{equ} (f_0) than the unloaded TL impedance Z_C. Thus, topology X should be selected if the minimum host impedance Z_C achievable in the technology considered is larger than the desired Z_G (see the example of Section 5). In contrast, topology Y must be selected if the technology does not allow sufficiently high unloaded TL impedance values.
ii. Some inspection of (8) shows that the difference between Z_{equ} and Z_C is only significant if the condition (5) is not met. As explained in Section 2, this condition is equivalent to $d \ll \lambda_0$ for balanced CRLH-TLs based on the unit cell circuits shown in Figure 1. As a result, we can only extend the range of achievable impedance Z_G much beyond the limit of the technology Z_C in the case where $d \ll \lambda_0$ is not true, which means that "conventional " CRLH-TL design strategies based on this assumption would not allow designing low or high impedances as done here. It is noticeable that this observation is coherent with the result of Section 2 that $Z_{equ,X/Y}$ (f_0) = Z_C in the case where $d \ll \lambda_0$, as was already observed in works whose developments are based on this assumption [2, 3].

Finally, let us recall that as explained in [4, 5], CRLH-TLs that do not verify $d \ll \lambda_0$ are still useful to most CRLH-TL applications, whether in the case of phase shifting-based devices such as series feed networks [3] or couplers [2], or in applications involving a transmission between the structure and surrounding media (e.g. leaky-wave antennas, focusing [6]).

4. APPLICATIONS

The range of achievable unloaded impedances in conventional technologies is usually limited, due to fabrication or space constraints (see Section 5). However, we showed that it is possible to achieve Bloch impedances Z_{equ} (f_0) higher or lower than the impedance Z_C of the unloaded TL sections in the CRLH-TL by using a noneffectively homogeneous CRLH-TL and appropriate design expressions. As a result, two main fields of applications can be envisioned for the results presented in this letter.

The first one concerns applications based on the CRLH-TL particular dispersion characteristic. In this case, the method allows designing CRLH-TLs with an extended impedance range when compared with usual CRLH-TLs (for which we showed that Z_{equ} (f_0) is necessarily equal to Z_C). For example, this would allow controlling the impedance of the different line sections in a CRLH-TL-based series feed network for optimal matching [3]. Similarly, a slab of metamaterial embedded in air for focusing application should exhibit the free space impedance of 377 Ω for optimal matching.

Second, the CRLH-TL can be used to mimic low or high impedance conventional—or true-time delay—TLs. For instance, a matching network might require impedance values not achievable in a given technology; this problem can be overcome by using a CRLH-TL and the presented design procedure. It is however worth mentioning that the CRLH-TL dispersion is different from a conventional TL; thus, it cannot be used to mimic a conventional TL in all applications. However, as will be seen in Section 5, a balanced CRLH-TL as designed here exhibits a linear phase shift on a wide BW and can therefore be used in most applications in this second category.

5. DEMONSTRATOR

Depending on the substrate characteristics, process resolution, and the type of waveguide (e.g. CPW, microstrip), it is usually difficult to realize either high or low characteristic impedance values. We provide here an example where it is especially hard to achieve a low impedance and demonstrate how this limitation is overcome by the appropriate CRLH-TL design.

5.1. Design

We consider here the case of CPW-based structures integrated on quartz ($\varepsilon_r = 3.8$). The total width of the CPW is set to $G + 2W = 1000$ μm, where G and W are the width of the central conductor and the slots of the CPW, respectively. If we want to realize a 20-Ω CPW in this technology, this means that the slots width G must be only about 0.3 μm which is not a realistic value in a conventional process (e.g [7]). Even in the case of an impedance of 30 Ω, the slot would have to be 6-μm wide, which is also critical from a precision point-of-view. Although there are some techniques to obtain low-impedance TL, they are based on sophisticated multilayer fabrication processes. Thus, we will employ the method presented here to design a 20-Ω CRLH-TL based on the aforementioned single-layer technology and CPW size.

First, let us observe from (9) that topology X of Figure 1 should be selected in order to realize a CRLH-TL with a lower impedance $Z_{equ,X}(f_0) = Z_G$ than the achievable unloaded TL impedance Z_C. We continue the design by choosing $L_P = 120$ pH and consider the design targets $f_0 = 15$ GHz and $Z_G = 20$ Ω. Using (3), we obtain $C_{S,X} = 65.4$ fF. Finally, the impedance $Z_C = 42.8$ Ω and length $d/2 = 2.27$ mm of the unloaded TL sections are found using (1) and (2), respectively. Both L_P and $C_{S,X}$ lumped element values are then translated into layouts using full-wave simulations and extraction procedures [4]. A good precision is required in this process for final structure to exhibit expected performances. As expected, we can verify that conditions $d \ll \lambda_0$ and (5) are not verified; indeed, as explained previously, only a CRLH-TL that is not effectively homogenous allows achieving a Bloch impedance $Z_G = 20$ Ω significantly smaller than the host TL impedance $Z_C = 42.8$ Ω (which is easily realized with a conventional precision).

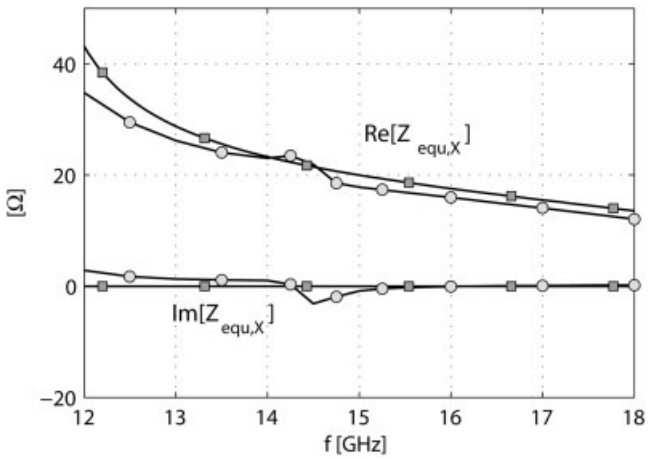

Figure 2 Bloch wave impedance of the designed CRLH-TL. Squares: ideal circuit model, Circles: full-wave simulation

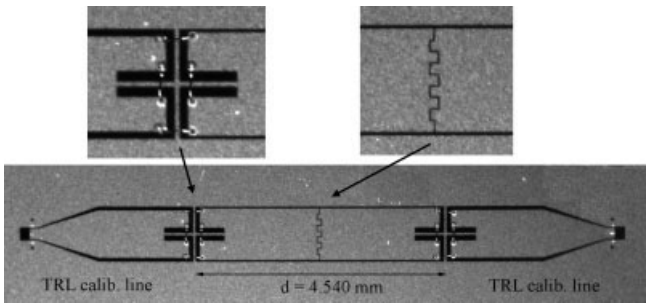

Figure 3 Picture of the fabricated type X 1-cell low-impedance CRLH-TL. The loading shunt inductance (incl. wirebond bridges) and series capacitance are shown in the left and right insets, respectively

Figure 2 shows the resulting Bloch wave impedance $Z_{equ,X}$ on a wide BW around $f_0 = 15$ GHz. First, the results for the circuit of Figure 1 with the above design values show that the impedance is exactly 20 Ω at f_0 and smoothly varying with frequency. As no losses are considered in the circuit, the imaginary part of the impedance is exactly zero. The graph also shows the HFSS full-wave simulation results on the exact designed structure. A good agreement is observed, despite some discrepancies due to the losses and parasitics of the actual simulated structure, which were for simplicity not induced in the circuit here.

5.2. RESULTS

Figure 3 shows the designed low-impedance CRLH-TL made of micromachined aluminium on a quartz wafer. We present here the results for a single unit cell, since the properties of a CRLH-TL with any number of cells can be easily deduced from the measurement of its unit cell using Bloch wave parameters [4].

The measurements were taken on-wafer using a through-reflect-line (TRL) calibration with 50-Ω reference CPW lines (see Fig. 3). The reference impedance of the S-parameter was then changed from 50 to 20 Ω. These measurements are shown in Figure 4 and compared with full-wave simulations using Ansoft HFSS, which were also simulated using 50 Ω CPW "waveports" ports subsequently renormalized to 20 Ω.

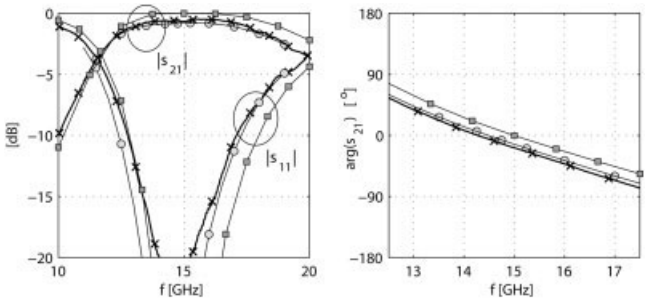

Figure 4 S-parameters of the low-impedance CRLH-TL with a reference impedance of 20 Ω. Squares: ideal circuit model, Circles: full-wave simulation, Crosses: measurement

An excellent agreement between full-wave simulations and measurements is observed. These results slightly differ from the ideal circuit model results since no losses and parasitics elements were introduced here in the circuit. The measured −10-dB matching BW is almost 5 GHz around the $f_0 = 15$-GHz target frequency, which corresponds to a 30% BW. This means that the Bloch wave impedance is close to 20 Ω on a wide band, as suggested by Figure 2. The measured insertion loss is −0.6 dB on a 17% BW and is better than −1 dB on the whole matching BW. The right-hand side of Figure 4 shows the phase shift within the BW (12.5–17.5 GHz); an excellent phase shift continuity at f_0 is achieved, as well as good phase linearity within the whole band.

REFERENCES

1. M. Gil, I. Gil, J. Bonache, J. García-García, and F. Martín, Metamaterial transmission lines with extreme impedance values, Microwave Opt Technol Lett 48 (2006), 2499–2505.
2. I.-H. Lin, M. DeVincentis, C. Caloz, and T. Itoh, Arbitrary dual-band components using composite right/left-handed transmission lines, IEEE Trans Microwave Theory Tech 52 (2004), 1142–1149.
3. M.A. Antoniades and G.V. Eleftheriades, A metamaterial series-fed linear dipole array with reduced beam squinting, IEEE Int Symp Antennas Propag, Albuquerque, NM (2006), 4125–4128.
4. J. Perruisseau-Carrier and A.K. Skrivervik, Composite right/left handed transmission line metamaterial phase shifters (MPS) in MMIC technology, IEEE Trans Microwave Theory Tech 54 (2006), 1582–1589.
5. J. Perruisseau-Carrier and A.K. Skrivervik, A bloch wave approach to the design of optimally matched non-effective medium composite right/left handed transmission lines, IEE Proc Microwaves Antennas Propag, submitted.
6. D.R. Smith, S. Schultz, P. Markoš, and C.M. Soukoulis, Experimental verification of a negative index of refraction, Science 292 (2001), 77–79.
7. Y. Kwon, H.-T. Kim, J.-H. Park, and Y.-K. Kim, Low-loss micromachined inverted overlay CPW lines with wide impedance ranges and inherent airbridge connection capability, IEEE Microwave Wireless Compon Lett 11 (2001), 59–61.

© 2007 Wiley Periodicals, Inc.

COMPACT MICROSTRIP BANDPASS FILTER USING COMPOSITE RIGHT/LEFT-HANDED TRANSMISSION LINES

Jiusheng Li[1,2] and Zhuang Yunyun[2]

[1] Centre for THz Research, China Jiliang University, Hangzhou 310018, People's Republic of China

[2] School of Electronics and Information Engineering, China Jiliang University, Hangzhou 310018, People's Republic of China

Received 7 January 2007

ABSTRACT: *A compact microstrip bandpass filter utilizing composite right/left-handed (CRLH) transmission lines (TLs) is designed, fabricated, and measured. The simulated and measured results show that the proposed filter has low insertion loss in passband, compact dimensions, easy fabrication, and low cost. The novel measured performances of the bandpass filter based on CRLH TL are almost identical with the simulated results.* © 2007 Wiley Periodicals, Inc. Microwave Opt Technol Lett 49: 1929–1931, 2007; Published online in Wiley InterScience (www.interscience.wiley.com). DOI 10.1002/mop.22613

Key words: *composite right/left-handed (CRLH); transmission lines (TLs); left-handed (LH); bandpass filter*

1. INTRODUCTION

In the recent years, research on left-handed medium (LHM) with negative permittivity and negative permeability has become very active because of its many unusual physical properties different from the conventional right-handed (RH) material, such as the negative refraction index, the backward Cerenkov radiation, the reversed Doppler shift, etc. An extended concept of composite right/left-handed transmission line was developed and it demonstrated the practical application of left-handed (LH) structure in 2004 [1–3]. Following the experimental verification, LHM has become an attractive topic, and an extensive investigation has been conducted in the new physical characteristics, experiments, and potential applications.

With the rapid development of microwave and millimeter wave communication systems [4], it greatly stimulates the demand on high performance microwave filters with compact dimensions, low insertion loss, high attenuation in stop band, and low cost. Various configurations of bandpass filters have been developed to meet the above goal in the past few decades [5–11]. But most of the presented designs are still unsuitable for miniaturized realization. To tackle this problem, some filters using photonic bandgap and defect ground structures have been proposed [12, 13]. These approaches lead to a complex design procedure and are unsuitable for integration.

To further reduce the filters circuitry size and obtain high performance microwave filter, a novel compact bandpass filter using composite right/left-handed (CRLH) transmission lines (TL) unit cells is developed in this letter. The proposed filter constituted of CRLH TL that can easily be realized using printed circuit technology. The novel device is easily integrated with microwave or millimeter wave planar circuits. The novel bandpass filter has low passband insert loss, compactness, and excellent stop band attenuation, etc. The performances of the bandpass filter are demonstrated by the simulation and measurement results. The measurement results closely correspond to the theoretical predictions is observed.

2. COMPACT FILTER DESIGN

The configuration of the proposed filter based on CRLH TL and its equivalent circuit are shown in Figure 1. In our design, we assume that the structure is lossless and the width of the feeding lines is negligible. Two 50 Ω feedings are added at the filter input and

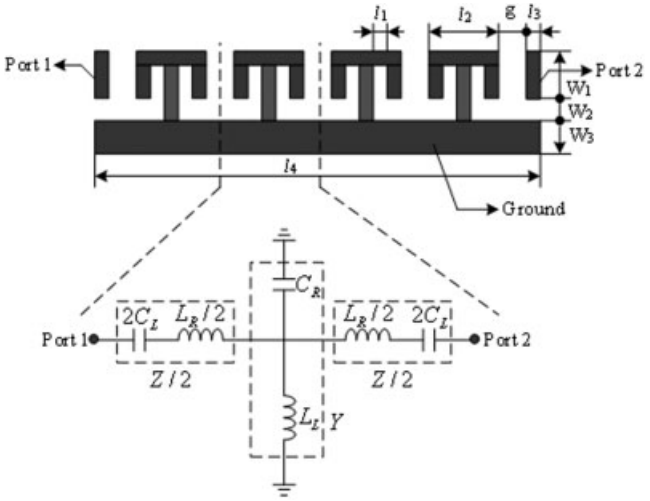

Figure 1 Sketch of the novel microstrip filter using CRLH TL and CRLH TL unit cell